BRD4 Prevents R-Loop Formation and Transcription-Replication Conflicts by Ensuring Efficient Transcription Elongation

Drake Edwards[1-3], Rohin Maganti[4], Jarred P. Tanksley[3], James J.H. Park[3], Elena Balkanska-Sinclair[3], Jie Luo[3], Jinjie Ling[4] and Scott R. Floyd[2,3]*

[1]Medical Scientist Training Program, Duke University School of Medicine, Durham, North Carolina 27710, USA
[2]Department of Pharmacology and Cancer Biology, Duke University Medical Center, Durham, North Carolina 27710, USA
[3]Department of Radiation Oncology, Duke University School of Medicine, Durham, North Carolina 27710, USA
[4]Duke University, Durham, North Carolina 27710, USA

*Corresponding author:
Scott R. Floyd
Levine Science Research Center, Rm B233
450 Research Drive
Durham, NC 27510
919-684-9337
scott.floyd@duke.edu

ABSTRACT

Effective spatio-temporal control of transcription and replication during S-phase is paramount to maintain genomic integrity and cell survival. Deregulation of these systems can lead to conflicts between the transcription and replication machinery leading to DNA damage. BRD4, a BET bromodomain protein and known transcriptional regulator, interacts with P-TEFb to ensure efficient transcriptional elongation by stimulating phosphorylation of RNA Polymerase II (RNAPII). Here we report that disruption of BET bromodomain protein function causes DNA damage that correlates with RNAPII-dependent transcript elongation and occurs preferentially in S-phase cells. BET bromodomain inhibition also causes accumulation of RNA:DNA hybrids (R-loops), which are known to lead to transcription-replication conflicts, DNA damage, and cell death. Furthermore, we show that resolution of R-loops abrogates BET-bromodomain inhibitor-induced DNA damage, and that BET-bromodomain inhibition induces both R-loops and DNA damage at sites of BRD4 occupancy. Finally, we see that the BRD4 C-terminal domain, which interacts with P-TEFb, is required to prevent R-loop formation and DNA damage caused by BET bromodomain inhibition. Together, these findings demonstrate that BET bromodomain inhibitors can damage DNA via induction of R-loops in highly replicative cells.

INTRODUCTION

Maintaining the integrity of the genome throughout the cell cycle is paramount to cell survival[1], and therefore complex systems have evolved to tackle various threats to the genome's integrity[2-4]. During S-phase, areas of chromatin that are engaged with generating RNA transcripts must be coordinated with migrating replication forks. Disruption of either transcription or replication control and coordination can lead to the desynchronization of these chromatin-based activities, resulting in transcription-replication conflicts (TRCs) and subsequent replication stress, DNA damage, and cell death[5-9]. To avoid these collisions, these processes are separated in both time and space through the activity of several known chromatin-based complexes[3]. Specifically, the processivity of both the replication machinery and the nascent RNA strand are paramount in preventing collisions between the two[10,11]. These systems are an active area of study, especially in cancer cells, as many amplified transcription programs and more frequent replication distinguish cancer cells from normal cells[12,13]. The strategies that cancer cells employ to avoid TRCs are therefore of potential therapeutic interest, as the components of these TRC avoidance mechanisms could be targeted with wide therapeutic window in variety of cancers.

One source of TRCs is the aberrant formation of RNA:DNA hybrids (R-loops), caused by nascent RNA re-annealing with its DNA template strand forming a three-stranded structure[3,5,9,14-19]. R-loops play various physiological roles, including Ig class-switching, CRISPR-Cas9 bacterial defense systems, and normal transcription regulation[14,20-25]. However, pathologic R-loops can also form from dysregulated transcription, and these pathologic R-loops can impede the progression of the

transcription bubble[15]. In the case where RNAPII is stalled, the nascent RNA is allowed to re-anneal with its template strand and form a stable R-loop leading to tethering of RNAPII to the chromatin. During S-phase, these R-loop-tethered transcription bubbles create a roadblock for replication forks[26,27]. If these roadblocks are not resolved, collisions with the replication machinery will lead to replication fork breakdown and DNA strand breaks. Important factors have been identified that prevent and resolve R-loops, including the RNAPII activator CDK9 and the RNA:DNA hybrid endonuclease RNase H1[27-37].

BRD4, a member of the bromodomain and extra-terminal domain (BET) protein family, is a known regulator of transcription elongation. Through its C-terminal domain (CTD) it is known to activate CDK9, the RNAPII-phosphorylating component of the positive transcription elongation factor, P-TEFb[38-46]. After RNAPII has initiated transcription and paused, at many genomic loci, BRD4 releases P-TEFb from its inhibitory complex and allows CDK9 to phosphorylate the second serine of the YSPTSPS repeat on the tail of RNAPII (RNAPIIpS2). Once this phosphorylation event occurs, RNAPII is able to enter the elongation phase of transcription. Consequently, inhibition of BRD4 function reduces transcription of many transcripts[38,47-49].

BET family inhibitors have shown activity in pre-clinical models of several cancers, and clinical trials have shown efficacy, yet mechanisms of action and predictive biomarkers remain elusive. In an effort to illuminate the role BRD4 plays in preventing cancer cell death, we have studied how the DNA damage repair systems react to BET inhibition. We see that BET inhibitors cause double strand breaks in cells undergoing S-phase replication. Furthermore, we see that overexpression of full-length

BRD4 rescues the effects of BRD4 loss, but rescue fails when BRD4 is truncated to delete the P-TEFb-interacting C-terminal domain (CTD). Finally, we see that BET inhibitors cause an increase in the formation of R-loops and that overexpression of RNase H1, an endonuclease that acts on the RNA strand of R-loops, reverses BET inhibitor-induced DNA damage. These data suggest a new role for BRD4 in preventing aberrant R-loop formation and TRCs by ensuring efficient RNAPII transcription.

RESULTS

Inhibition or degradation of BET family proteins leads to spontaneous DNA damage in cancer cells

BRD4, through its two N-terminal bromodomains, interacts with the chromatin by binding to acetylated histones[50]. In previous work, we have described how a low abundance isoform of BRD4 (Isoform B) mediated chromatin dynamics and DNA damage signaling in the presence of radiation[51]. However, small molecule BET bromodomain protein inhibitors are effective against cancer cells in the absence of radiation[52-55]. Several groups have reported variable effects of BET bromodomain inhibitors on DNA damage signaling[56-60]. We therefore sought to understand the DNA damage consequences of BET bromodomain inhibition. JQ1, a small molecule inhibitor of BET family proteins, binds to the bromodomains and competitively prevents BRD4 from interacting with chromatin[49]. In order to test whether JQ1 was able to induce a DNA damage response, we treated HeLa and HCT-116 cells with high dose (500 nM) JQ1 for 16 hours and stained for γH2AX foci, a marker of DNA damage[61]. Surprisingly, in contrast to what we and others observed in U2OS cells treated with low dose JQ1, we saw that JQ1 was able to induce γH2AX foci formation, indicating that BET proteins can prevent spontaneous DNA damage **(Fig. 1a, b, Supplementary Fig. 1A and Supplementary Fig. 1B)**.

Recently, a small molecule, dBET6, has been shown to cause rapid degradation of BET proteins[38]. dBET6, as with other PROTAC molecules, links JQ1 to an E3-ligase recruiter which causes ubiquitination and subsequent, rapid degradation of BET proteins. Advantages of dBET6 are that it allows for the visualization of BET protein loss

and acts as a more potent BET protein inhibitor with fast time kinetics. We observed that dBET6 elicited a robust DNA damage response detectable by Western blot in HeLa cells at 100 nM concentration in as few as 6 hours. Concurrent with dBET6-induced loss of BET proteins, we observed a reduction in RNA Polymerase II phospho-Serine 2 and saw γH2AX signaling both by western blot and immunofluorescence **(Figure 1c, d, and e)**. These observations confirmed that loss of BET proteins result in increased DNA damage signaling.

While γH2AX is a general marker for DNA damage signaling, we wanted to establish whether BET protein loss also leads to an increase in physical DNA damage such as double strand breaks. We therefore employed single cell electrophoresis (comet assay) to measure the amount of DNA double strand breaks after dBET6 treatment. Interestingly, we found that in addition to the DNA damage signaling increase, dBET6 increased the number of DNA double strand breaks **(Figure 1f and g)**. These observations indicate that loss of the BET family of proteins can cause physical DNA damage as well as a robust DNA damage response.

BET protein loss induces DNA damage during S-phase

Transcription-replication conflicts, by definition, occur while the cell is actively replicating its genome during S-phase. An active replication fork, when it collides with a transcription bubble in the head-on orientation, leads to fork stalling, DNA damage, and cell death[17]. While probing for DNA damage following BET protein loss, in immunofluorescence microscopy studies, we noticed heterogeneity in which cells would display γH2AX foci following dBET6 exposure. Prior work from other groups showed

that BRD4 loss leads to a loss of S-phase cells[62]. While this has been described as a G1/S phase arrest, we decided to determine whether actively replicating S-phase cells could be prone to DNA damage after BRD4 loss.

To test whether BET protein loss leads to DNA damage preferentially in actively replicating cells, we labeled HeLa cells with EdU to monitor actively replicating cells while simultaneously treating with BET6 for two hours. Our hypothesis was that, if BET protein loss is leading to TRCs, that S-phase cells that are actively replicating would preferentially exhibit a DNA damage response. Accordingly, we observed that γH2AX foci formed only in the cells that were labeled with EdU by immunofluorescence **(Fig. 2a and b)**. We also labeled OCI-AML2 cells, another JQ1 sensitive cell line[63,64], and also saw that EdU positive cells showed the most DNA damage following dBET6 treatment **(Supplementary Fig. 2A and Supplementary Fig. 2B)**. These data indicate that BET protein loss is specifically leading to DNA damage in cells that are actively replicating in S-phase.

To determine whether this S-phase-specific DNA damage was resulting in a loss of cells in S-phase, we analyzed the cell cycle of HeLa cells treated with JQ1 or dBET6. As shown in **Fig. 2c,** we saw that both JQ1 and dBET6 led to a decreased proportion of cells in S-phase, suggesting that BET protein loss leads loss of replicating cells.

The observation that BET protein loss was causing DNA damage in S-phase led us to suspect that BET inhibitor-treated cells were under replication stress. To test this, we measured phosphorylation of RPA2, a downstream target of the replication stress master kinase ATR. RPA2 is known to be phosphorylated on Serine 33 (RPA2-pS33) by ATR in response to replication stress[65]. BET inhibition with dBET6 caused a robust

increase in RPA2-pS33 **(Figure 2d)**, indicating that BET inhibition causes replication stress, and providing further evidence that BET protein loss leads to TRCs.

The C-Terminal Domain of BRD4 is necessary to prevent DNA damage caused by BET protein loss

The BET protein family consists of four members: BRD2, BRD3, BRD4, and BRDT, (of note, BRDT is expressed mainly in the testes)[66]. Inhibitors of this family of proteins, namely JQ1 and the degrader dBET6, function by binding to the bromodomains which are shared by all members. Thus, it is important to elucidate which member is responsible for the DNA damage seen by dBET6 treatment. To test this, we used siRNA to knock down BRD2, BRD3, and BRD4 and measured γH2AX signaling **(Fig. 3a and Supplementary Fig. 3A)**. After 72 hours of knock down, we observed that both BRD2 and BRD4 loss led to increased γH2AX signaling. Owing to a wealth of studies that established mechanisms of BRD4 in transcription regulation, and earlier work showing replication dysfunction caused by BRD4 loss[30,38,67,68], we focused on the role of BRD4 in the prevention of TRC-induced DNA damage.

The full-length isoform of BRD4, isoform A, contains several known domains, including two bromodomains, an extra-terminal domain, and a C-terminal domain **(Fig. 3b)**. The two bromodomains, which bind to acetylated lysine on histone tails, and the extra-terminal domain are shared among all BET protein members. The C-terminal domain, however, is unique to BRD4 isoform A and interacts with the P-TEFb complex that contains CDK9, leading to Serine 2 phosphorylation of RNAPII and transcription pause-release[38-46]. Also, previous work showed that CDK9 inhibition leads to an

increase in R-loop-induced stalled RNAPII and potentially TRCs[20,69]. Thus, we hypothesized that BRD4 loss could also lead to CDK9 dysfunction, resulting in TRCs and DNA damage. Moreover, we reasoned that the P-TEFb-interacting CTD would be required to prevent TRCs and DNA damage.

To determine the role of BRD4 in preventing damage caused by BET protein loss, we developed a panel of inducible BRD4 overexpression constructs in order to test their ability to rescue the effects of dBET6 **(Fig. 3b)**. The panel included two naturally occurring isoforms, A and C. Isoform A being the full length isoform mentioned above, and isoform C as a shorter isoform only including the two bromodomains and the extra-terminal domain[56] (and lacking the CTD). We also developed a truncated construct of isoform A missing only the CTD (AΔCTD) which has previously shown to interact with CDK9[68]. Finally, we developed a construct excluding the extra-terminal domain (CΔET). These constructs were used to develop stable cell lines under doxycycline control to overexpress the BRD4 isoforms **(Supplementary Fig. 3B)**.

In order to determine whether BRD4 isoform A (full length isoform) was able to rescue the DNA damage effects caused by dBET6, we induced isoform A expression with doxycycline for 24 hours before treatment with dBET6. We found that isoform A was indeed able to rescue the γH2AX signaling caused by dBET6 **(Fig. 3c, d, and Supplementary Fig. 3C)**. While, we saw that isoform A was able to rescue the effects of dBET6 treatment, the protein levels of overexpression construct remaining after dBET6 treatment were difficult to detect by Western blot. To further verify rescue of TRC-induced DNA damage by BRD4 isoform A, we measured BRD4 levels by immunofluorescence staining of dBET6-treated cells that either did, or did not, contain

the overexpression construct **(Supplementary Fig. 3D)**. As expected, isoform A was still present after dBET6 treatment only in cells expressing the induced rescue construct, confirming that the rescue of γH2AX was due to isoform A still being present. We also observed that isoform A was able to rescue the loss of RNAPIIpS2, indicating that overexpressing full-length BRD4 was able to ensure efficient transcription elongation even in the presence of dBET6. These data suggest that BRD4 is sufficient in rescuing the effects of dBET6. Next, we applied the same conditions to the entire panel of BRD4 overexpression constructs by western blot **(Fig. 3c and d)**. Importantly, none of the other overexpression constructs was able to rescue either the γH2AX signaling or the loss of RNAPIIpS2. Furthermore, we saw that only isoform A was able to rescue the S-phase specific γH2AX foci caused by dBET6 treatment **(Fig. 3e and f)**. These observations indicate that the C-terminal domain (CTD) is required to prevent BET inhibitor-induced loss of RNAPIIpS2, TRC, and DNA damage.

Next, we wanted to elucidate whether the CTD of BRD4 was necessary to rescue the DNA double strand breaks caused by dBET6 treatment. To test this, we used a comet assay to quantify the breaks following dBET6 treatment following overexpression of isoform A or AΔCTD. Again, we saw that isoform A, but not AΔCTD, was able to rescue the dBET6-induced DNA double strand breaks. This further indicates that the C-terminal domain of BRD4 is necessary to prevent spontaneous TRCs and subsequent DNA double strand breaks.

BET inhibition leads to an increase in R-loop-dependent DNA damage

R-loops have been previously shown to cause transcription-replication conflicts and replication stress in cancer[3,5,9,14-19]. Specifically, an R-loop is able to tether a stalled RNAPII to the chromatin upon which becomes a roadblock for replication machinery. RNAPII, after initiation of transcription of ~50 bp, becomes paused until a second phosphorylation event of the second serine on its tail. BRD4, through its C-terminal domain, activates CDK9 to undergo this phosphorylation event and ensure efficient transcription elongation[40,41,43,46,68,70]. Previous work has also shown that loss of BRD4 leads to decreased traveling ratios of RNAPII after dBET6 treatment, indicating that RNAPII is stalled on the chromatin[38]. Furthermore, previous studies have indicated that direct chemical inhibition of CDK9 leads to stalled RNAPII and an increase in R-loop formation[21,28]. Therefore, we hypothesized that loss of BRD4 may also lead to an increase of R-loops, and that those R-loops are responsible for the TRCs seen after BRD4 loss.

To determine whether BRD4 loss leads to an increase in R-loop formation, we employed the R-ChIP-seq technique which has previously been described as a way to view R-loop formation on the chromatin[69]. R-ChIP employs the use of a catalytically inactive form of the R-loop-specific endonuclease, RNase H1. The mutation, D210N, allows RNase H1 to bind to, but not resolve, R-loops. The construct is tagged with a V5 peptide, which then allows it to be enriched from crosslinked cells, along with associated chromatin, for ChIP-sequencing **(Supplementary Fig. 4A)**. We performed R-ChIP-seq in dBET6-exposed cells and found dramatic increases in global R-loop formation **(Fig. 4a)**. Similarly, we saw globally-increased γH2AX ChIP signal in dBET6-treated cells. Furthermore, we validated three previously described[42] BRD4 occupying

loci using R-ChIP-qPCR **(Fig. 4b and c)**. Surprisingly, while we saw most of the R-loop formation near the promoter regions, there was also increased R-loop formation throughout the length of the gene. In addition, we also saw a decrease of RNAPIIpS2 along the length of these loci as well **(Supplementary Fig. 4B)**. This indicates that BRD4 not only prevents pause-release of RNAPII, but also prevents the accumulation of R-loops and RNAPII stalling throughout the length of the gene.

We next postulated that the R-loops formed by BRD4 loss would be the cause of the TRCs, replication stress, and DNA damage. To elucidate this, we employed the overexpression of V5-tagged wild-type RNase H1, which is known to be able to resolve R-loops and reverse DNA damage caused by their existence[27]. As a negative control, we used a V5-tagged RNase H1 mutant, containing mutations at W43A, K59A, K60A and D210N (WKKD), which has been previously described to lack both the catalytic activity as well as the DNA binding activity of RNase H1[28]. To test whether RNase H1 was able to rescue the TRCs caused by BRD4 loss, we overexpressed either the WT RNase H1 or the WKKD mutant construct, treated with dBET6, and stained for V5, EdU, and γH2AX **(Fig. 4d, e, and Supplementary Fig. 4C)**. Consistent with our hypothesis that BET inhibition leads to TRC and DNA damage via increased formation of R-loops, over-expression of WT RNaseH1, but not the non-binding WKKD mutant, rescued the DNA damage induced by BRD4 loss in EdU positive cells. We then sought to test whether RNase H1 was able to rescue the DNA double strand breaks caused by dBET6 **(Fig. 4f and g)**. We observed that RNase H1 was also able to rescue these DNA double strand breaks. These data indicate that following BRD4 loss, R-loops are formed and lead to TRCs and subsequent DNA damage.

Finally, because BRD4 plays a role in transcription, we sought to understand whether BRD4 was playing a direct role in preventing R-loop formation, or whether it was indirectly preventing R-loop formation through the transcriptional control of other proteins implicated in R-loop processing. SETX and SRSF1 have both been previously shown to be involved with R-loop processing[71,72]. We saw that dBET6 treatment did not impact the level of neither SETX nor SRSF1 in the timeframe when the R-loop-dependent TRCs and DNA damage occurred **(Fig. 4h)**.

Active transcription and RNAPII occupancy are required for BET protein-loss induced damage

There are five stages of transcription: RNAPII recruitment, initiation, pause/release, elongation, and termination[73,74]. Transcription initiation is denoted by a phosphorylation event, namely that CDK7, a subunit of TFIIH, phosphorylates Serine-5 on the tail of RNAPII[75]. After ~50bp of nascent transcription, RNAPII undergoes a pausing event until CDK9, a subunit of P-TEFb, phosphorylates Serine-2 on the tail of RNAPII[76]. Inhibitors of these two kinases exist and have been shown to have different effects on RNAPII occupation of chromatin[21]. Triptolide (TRP) inhibits CDK7 and results in the blocking of transcription initiation and leads to the degradation of RNAPII **(Supplementary Fig. 5A)**. DRB inhibits CDK9 and leads loss of RNAPIIpS2 and stalling of RNAPII on the chromatin, resulting in R-loops and TRCs[28,77] **(Supplementary Fig. 5B)**. With this understanding, we hypothesized that these two molecules would have differing effects on the DNA damage caused by BRD4 loss.

To test whether degradation of RNAPII with TRP would be able to rescue the DNA damage effects of dBET6 treatment, we designed an experiment to pre-treat and manipulate RNAPII prior to dBET6 exposure, as described in **Figure 5a**. After pre-treating with either TRP or DRB, we washed out the drugs and treated with dBET6 for one hour. Following the dBET6 treatment, cells were fixed and stained for γH2AX **(Fig. 5b and c)**. Remarkably, we saw that TRP was able to rescue the DNA damage effects of dBET6, while DRB was not. We also co-treated TRP and dBET6 in HCT-116 cells and also saw that TRP was able to rescue the DNA damage effects caused by dBET6 **(Supplementary Fig. 5C and Supplementary Fig. 5D)**. These data indicate that RNAPII occupation on the chromatin is necessary for DNA damage caused by BRD4 loss.

Finally, we wanted to explore the correlation between RNAPIIpS2 and DNA damage caused by dBET6 treatment. We observe that when BRD4 isoform A is overexpressed, there is an increase in RNAPIIpS2 **(Fig. 5d)**. In addition, we see that RNAPIIpS2 negatively correlates with γH2AX following dBET6 treatment both in HeLa cells and HEK-293T cells **(Fig. 5e, f, Supplementary Fig. 5E, Supplementary Fig. 5F)**. These data again suggest that the loss of BRD4 leads to loss of transcription and stalling of RNAPII on the chromatin leading to TRCs and subsequent DNA damage.

DISCUSSION

Inhibitors of BRD4 have been shown to be effective treatments for several cancers, yet the mechanism of action remains unclear[52-55]. Specifically, questions remain as to why inhibition of BRD4, which controls global transcription[38], may preferentially impact cancer cells more than normal cells – a feature that is required of all effective chemotherapies. Here, we propose a novel role for BRD4 in the prevention of R-loops, transcription-replication conflicts, and DNA damage **(Figure 6)**.

Our data show that inhibition or degradation of BET proteins, with JQ1 or dBET6 respectively, leads to an accumulation of DNA damage signaling and DNA double strand breaks. When we began to characterize the nature of the DNA damage, we also noticed that the cell cycle state dictated whether or not they accumulated this damage. Specifically, we saw that the damage was S-phase specific. Due to our data and the literature showing that BET proteins play a role in transcription, we postulated that the S-phase dependent DNA damage caused by BET protein loss could be working through a mechanism of increased transcription-replication conflicts.

Due to the fact that BET protein inhibitors such as JQ1 and degraders such as dBET6 target the bromodomains of BRD2, BRD3, and BRD4, it is unclear if one member of the family is responsible for the DNA damage caused by BET protein loss. Several works have shown unique properties of each[78-80], they also share some redundant functions. Our data show that while both BRD2 and BRD4 show increased γH2AX signaling after 72 hours, we saw that overexpression of the full-length isoform (isoform A) was able to effectively rescue the DNA damage effects of BET protein

degradation by treatment with dBET6. Furthermore, we observed that the C-terminal domain of BRD4 was necessary to rescue this effect.

Our data and the literature show that the C-terminal domain plays a critical role in the activation of RNAPII to ensure efficient elongation[38-46]. BRD4, through its C-terminal domain, interacts with CDK9 to phosphorylate Serine-2 on the heptapeptide repeat on the tail of RNAPII. This phosphorylation event allows RNAPII to proceed with transcription elongation on schedule. Our data is in line with other studies that show that inhibition of either BRD4 or CDK9 leads to R-loop formation on the chromatin[28]. R-loops then are able to tether RNAPII to the chromatin and increase the likelihood of collisions with the replication machinery during S-phase.

In recent years, the importance of R-loops has become more apparent. While they play critical roles normal physiological activity[14,20-25], it has also come to light that aberrant R-loops can lead to transcription-replication conflicts, DNA damage, and cell death[3,5,9,14-19]. Our data show that BRD4 loss leads to an increase in R-loop formation on the chromatin, and the damage seen following BRD4 loss can be rescued by overexpressing RNase H1, an endonuclease that resolves R-loops. These observations indicate that BRD4 is important to cancer cells in that ensuring efficient transcription during S-phase prevents R-loop dependent conflicts between transcription and replication. We believe this is an important observation because cancer cells are generally replicating and transcribing more than normal cells, thus may be more dependent on BRD4 to prevent the transcription and replication machinery from colliding. This finding might also shed light on additional prior studies. Early work on BRD4 knockout mice showed both embryonic lethality and replication deficits [67,81].

Additionally, studies of the normal tissue toxicities of whole-animal knockout of BRD4 could indicate vulnerability in rapidly replicating normal tissues[82]. One outstanding question that remains to be completely resolved is what makes a cancer cell more or less sensitive to BRD4 loss. It has been shown that certain cancer cell lines are more sensitive to BET protein inhibition[52], yet it is unclear as to why this is the case. For example, our group and others have shown that BRD4 loss in U2-OS cells does not result in an increase in signaling [56,59]. Notably, it is reported that that U2-OS cells do not exhibit a decrease in RNAPIIpS2 following BRD4 loss[59]. As is well known, different cells operate under different transcriptional programming. We hypothesize that certain cancer cell lines may be more globally dependent on BRD4-mediated transcriptional activation, leading to R-loops, TRC and DNA damage upon BET inhibition. Specifically, we hypothesize that RNAPIIpS2 loss after BRD4 degradation could be predictive of whether a cancer cell line exhibits DNA damage following treatment. Through further study of both BRD4 and the role of R-loops in cancer, we hope that we can identify new chemotherapeutic targets and broaden the effectiveness of BET inhibitors in cancer therapies.

FIGURE LEGENDS

Figure 1: BET protein loss of function leads to spontaneous DNA damage.

a. Representative images and **b.** quantification of γH2AX staining per nucleus in HeLa cells treated with DMSO or 500 nM JQ1 for 16 hours (>100 cells). **c.** Representative western blots from HeLa cells treated with DMSO or 100 nM dBET6 for 6 hours before harvest: lysates are probed for the epitope indicated beside each panel. **d.** Representative images and **e.** quantification of γH2AX staining per nucleus in HeLa cells treated with DMSO or 100 nM dBET6 for 6 hours. **f.** Representative images and **g.** quantification of neutral single cell electrophoresis assay of HeLa cells treated with DMSO or 100 nM dBET6 for 6 hours. Student's t-test (two-tailed, unpaired) was performed on **b, e, g**. Data represent the mean ±SEM. **P* < 0.05; ***P* < 0.01; ****P* < 0.001. Source data are provided as a Source Data file.

Figure 2: BET protein degradation leads to replication stress and S-phase-dependent DNA damage.

a. Representative images and **b.** quantification of γH2AX staining per nucleus in HeLa cells treated simultaneously with 100 nM dBET6 and 10 μM EdU for 2 hours. **c.** Cell cycle analysis of HeLa cells treated with DMSO, 500 nM JQ1, or 100 nM dBET6 for times as shown. Cells were fixed after treatment, stained with PI, and quantified for DNA content using flow cytometry. **d.** Representative western blot images of lysates from HeLa cells treated with DMSO or 100 nM dBET6 for 6 hours probed for the epitope indicated beside each panel. Student's t-test (two-tailed, unpaired) was performed on **b**.

Data represent the mean ±SEM. *P < 0.05; **P < 0.01; ***P < 0.001. Source data are provided as a Source Data file.

Figure 3: The C-terminal domain of BRD4 is required to prevent transcription-replication conflicts.

a. Representative western blots of HeLa cells treated with siControl, siBRD2, siBRD3, or siBRD4 for 72 hours and probed for the epitope indicated beside each panel. **b.** Domain structure of overexpression constructs depicting the location of the bromodomains, extra-terminal domain, and C-terminal domain of BRD4. **c.** Representative images and **d.** quantification of western blots from HeLa cells stably infected with each BRD4 construct and induced with doxycycline for 24 hours before being treated with 10 nM dBET6 for 6 hours and harvested: lysates were probed for the epitope indicated beside each panel. **e.** Representative images and **f.** quantification of γH2AX staining per nucleus in EdU-positive HeLa cells induced as in **d** and then simultaneously treated with 10 nM dBET6 and 10 μM EdU for 2 hours. **g.** Representative images and **h.** quantification of neutral single cell electrophoresis assay of HeLa cells induced as in **d** followed by treatment with DMSO or 10 nM dBET6 for 6 hours. Student's t-test (two-tailed, unpaired) was performed on **d, f, h**. Data represent the mean ±SEM. *P < 0.05; **P < 0.01; ***P < 0.001. Source data are provided as a Source Data file.

Figure 4: BET inhibition leads to an increase in R-loop-dependent DNA damage

a. Global ChIP-seq and R-ChIP-seq signal relative to input for HeLa cells treated with DMSO or dBET6 as shown. The right panel depicts how different colors represent the ChIP-seq or R-ChIP-seq signal relative to input. **b.** BRD4 ChIP-seq signal of select loci from ChIP-seq data published in Liu, et al. (2013) [42] **c.** Quantification of R-ChIP-qPCR at loci shown in **b** after treatment with DMSO or 100 nM dBET6. **d.** Representative images and **e.** quantification of γH2AX staining per nucleus in HeLa cells transfected with wild-type or WKKD mutant RNase H1 before being treated with 100 nM dBET6 or 10 μM EdU for 4 hours. **f.** Representative images and **g.** quantification of neutral single cell electrophoresis assay of HeLa cells transfected as in **e** before treatment with DMSO or 100 nM dBET6 for 6 hours. **h.** Representative western blot images from HeLa cells treated with DMSO or dBET6 for 6 hours: lysates were probed for the epitope indicated beside each panel. Student's t-test (two-tailed, unpaired) was performed on **e**. ANOVA was performed on **g**. Data represent the mean ±SEM. **P* < 0.05; ***P* < 0.01; ****P* < 0.001. Source data are provided as a Source Data file.

Figure 5: RNAPII loss rescues TRCs caused by BET inhibition

a. Depiction of experimental design. HeLa cells were treated with 250 nM Triptolide or 100 μM DRB for four hours before being washed out. Subsequently, cells were treated with 100 nM dBET6 for one hour before fixation. **b.** Representative images and **c.** quantification of γH2AX staining per nucleus from HeLa cells treated as described in **a.** **d.** Representative images of western blots from HeLa cells stably induced with the expression construct shown above each column for 24 hours: lysates are probed for the epitope indicated beside each panel. **e.** Representative images and **f.** quantification of

western blots from HeLa cells treated with 100 nM dBET6 for indicated times: lysates were probed for the epitopes indicated next to each panel. ANOVA was performed on **c**. Data represent the mean ±SEM. *$P < 0.05$; **$P < 0.01$; ***$P < 0.001$. Source data are provided as a Source Data file.

Figure 6: Model depicting the role of BRD4 in the prevention of R-loop-dependent TRCs

a. In normal conditions, BRD4 interacts with CDK9 to ensure the efficient phosphorylation of Serine-2 on the tail of RNAPII to release from transcriptional pause and allow transcription elongation. When BRD4 is inhibited or degraded by JQ1 or dBET6 respectively, RNAPII is unable to release from transcriptional pause or undergo elongation. This results in the build-up of R-loops which lead to transcription-replication conflicts and subsequent DNA damage.

Figure S1: BET protein loss of function leads to spontaneous DNA damage.

A. Representative images and **B.** quantification of γH2AX staining per nucleus in HCT-116 cells treated with DMSO or 500 nM JQ1 for 16 hours. Student's t-test (two-tailed, unpaired) was performed on **B**. Data represent the mean ±SEM. *$P < 0.05$; **$P < 0.01$; ***$P < 0.001$. Source data are provided as a Source Data file.

Figure S2: BET protein degradation leads to replication stress and S-phase-dependent DNA damage.

A. Flow cytometry distribution of EdU in cells that positively stained for γH2AX signaling. OCI-AML2 cells were treated with DMSO or dBET6 for 2 hours before fixation. **B.** Quantification of γH2AX staining per nucleus in OCI-AML2 cells treated simultaneously with 100 nM dBET6 and 10 μM EdU for 2 hours. Source data are provided as a Source Data file.

Figure S3: The C-terminal domain of BRD4 is required to prevent transcription-replication conflicts.

A. Representative western blot images of HeLa cells treated with the described siRNA for 72 hours: lysates are probed for the epitope as described beside each panel **B.** Snapgene files depicting the 2-vector iBRD4 system. Lentiviral, doxycycline-inducible BRD4 isoform A construct (left panel) and rtTA3 (right panel) were co-infected and selected by blasticidin and mCherry flow sorting to obtain a pure population. **C.** Representative western blot images of HeLa cells induced with doxycycline for 24 hours and then treated with increasing levels of dBET6 for 6 hours: lysates are probed for the epitope as described beside each panel. **D.** Representative images of HeLa cells harboring BRD4 Isoform A construct induced with doxycycline for 24 hours before being treated with 100 nM dBET6 for 4 hours. **E.** Representative images of HeLa cells harboring BRD4 Isoform C construct induced with doxycycline for 24 hours before being treated with 100 nM dBET6 for 4 hours. Source data are provided as a Source Data file.

Figure S4: BET inhibition leads to an increase in R-loop-dependent DNA damage

A. Western blot image depicting immunoprecipitation of RNase H1 D210N to validate V5 specificity. HEK-293T cells were induced with RNaseH1-D210N-V5 before harvest and immunoprecipitated with an anti-V5 or anti-IgG antibody and compared to input. **B.** ChIP-qPCR signal for RNAPIIpS2 following treatment of HeLa cells with DMSO or dBET6 for 2 hours at loci described in Fig. 3b and c. **C.** Western blot image confirming validation of wild-type or WKKD mutant RNaseH1-V5 constructs. Source data are provided as a Source Data file.

Figure S5: RNAPII loss rescues TRCs caused by BET inhibition

A. Western blot images of HeLa cells treated with DMSO or decreasing levels of triptolide for four hours: lysates probed for the epitope as described beside each panel. **B.** Western blot images of HeLa cells treated with DMSO or decreasing levels of DRB for four hours: lysates probed for the epitope as described beside each panel. **C.** Representative images and **D.** quantification of western blot images of HCT-116 cells treated with DMSO, 1 μM triptolide, and/or 100 nM dBET6 as described for four hours before harvest: lysates probed for the epitope described beside each panel. **E.** Representative images and **F.** quantification of western blots of HeLa cells treated with 100 nM dBET6 for indicated times: lysates probed for the epitope described next to each panel. ANOVA was performed on **D**.. Data represent the mean ±SEM. *$P < 0.05$; **$P < 0.01$; ***$P < 0.001$. Source data are provided as a Source Data file.

METHODS

Cell Culture

HeLa and HEK-293T cells were cultured in Dulbecco's modified Eagle's medium (DMEM) (Genesee Scientific) supplemented with 10% fetal bovine serum (FBS) (Summerlin Scientific Products) and 1% penicillin/streptomycin (P/S) (Thermo Fisher Scientific). HCT-116 cells were cultured in McCoy's 5A medium (Thermo Fisher Scientific) supplemented with 10% FBS and 1% P/S. OCI-AML2 cells were cultured in Roswell Park Memorial Institute 1640 medium (RPMI) (Thermo Fisher Scientific) supplemented with 10% FBS and 1% P/S.

Antibodies and stains

The following antibodies were used for western blot (WB), immunofluorescence (IF), or ChIP experiments: BRD4 N-terminus (1:1000WB, 1:1000IF, ab128874, Abcam); BRD2 (1:500WB, 5848S, Cell Signaling Technology); BRD3 (1:100WB, ab50818, Abcam); RNAPIIpS2 (1:1000WB, 1:50ChIP, 04-1571, EMD Millipore); γH2AX (1:1000WB, 1:1000IF, 1:50ChIP, 9718S, Cell Signaling Technology); α-Tubulin (1:1000WB, 2144S, Cell Signaling Technology); RPA2pS33 (1:500WB, ab211877, Abcam); V5 (1:1000IF, 1:50ChIP, ab9116, Abcam); SETX (1:500WB, ab220827, Abcam); SRSF1 (1:500WB, 324600, Thermo Fisher Scientific); Total RNAPII (1:000WB, 1:50ChIP, ab817, Abcam); Goat Anti-Rabbit IgG 800CW (1:6000WB, 926-32211, LI-COR Biosciences); Goat Anti-Mouse IgG 680RD (1:6000WB, 926-68070, LI-COR Biosciences); Goat Anti-Rat IgG 680LT (1:6000, 926-68029, LI-COR Biosciences); Goat Anti-Rabbit IgG Alexa Fluor 647nm (1:500IF, A211245, Life Technologies); Goat Anti-Rabbit IgG Alexa Fluor 555nm

(1:500IF, A21428, Invitrogen); Goat Anti-Rabbit IgG Alexa Fluor 488nm (1:500IF, A11008, Life Technologies).

DAPI (1:2000IF, Thermo Fisher Scientific) was used to stain nuclei. SYBR Gold (1X, Thermo Fisher Scientific) was used to stain single cell electrophoresis (comet) assay. Propidium Iodide (50 µg/mL, VWR) was used to stain nuclei for cell cycle analysis.

Immunofluorescence

Cells were grown on coverslips or in micro-chamber wells (Ibidi) overnight before induction or treatment. When the experiment was completed, cells were washed with ice cold PBS and fixed with 4% paraformaldehyde for 20 minutes at room temperature (RT). After fixation, cells were washed with PBS and then blocked in 5% goat serum and .25% Triton-X for 1 hour at RT, rocking. Following blocking, primary antibodies were diluted in the same blocking buffer and incubated at 4°C overnight, rocking. Following incubation with primary antibody, cells were washed three times with PBS and stained with the appropriate secondary antibody diluted and DAPI in blocking buffer at RT for 1 hour, rocking. After incubation with secondary antibody, cells were washed three times with PBS. In the case of cells grown on coverslips, cells were mounted on slides using Prolong Gold (Thermo Fisher Scientific) before imaging. Cells grown in micro-chamber wells were left in PBS before immediate imaging. Immunofluorescence images were taken either on a Zeiss Axio Observer or EVOS microscope using a 40X objective. Quantification of γH2AX foci was done using the speckle counting pipeline in CellProfiler. All images within a single experiment were fed into the same pipeline and

speckles (foci) were counted in an unbiased fashion using the automated program. γH2AX signal is defined as the multiplication of foci count of a nucleus with the mean integrated intensity of the foci within that nucleus.

Western Blotting

Whole cell lysates were prepared with a whole cell lysis buffer (50mM Tris-HCl pH 8.0, 10mM EDTA, 1% SDS) with protease and phosphatase inhibitors (Thermo, 78440) added fresh. Lysates were then sonicated using a QSonica Q700 sonicator for two minutes with an amplitude of 35. After sonication, protein concentrations were determined using BCA reagents (Pierce), compared to protein assay standards (Thermo Fischer Scientific), and scanned using a Spectramax i3x. Equivalent amounts of protein were resolved by SDS-PAGE gels and transferred to nitrocellulose membranes. Membranes were then blocked with a 1:1 solution of PBS and Odyssey Blocking Buffer (LI-COR Biosciences) at RT for one hour, rocking. Primary antibodies were then diluted in the blocking buffer as described above and incubated with the membranes at 4°C overnight. Membranes were then washed three times with 0.2% Tween-20 in PBS (PBS-T). The appropriate secondary antibodies were also diluted in the blocking buffer and incubated with the membranes at RT for one hour. Membranes were then washed with PBS-T three times and scanned using a LI-COR Odyssey scanner. Quantification and normalization of western blot signal was done using the LI-COR software, Image Studio.

Single Cell Electrophoresis (Comet) Assay

Neutral comet assays were performed using the CometAssay Reagent Kit (Trevigen) according to the manufacturer's protocol. Briefly, cells were washed in ice cold PBS, scraped from the plate, mixed with low melt agarose and spread onto supplied microscope slides in the dark. The agarose was gelled at 4°C for 30 minutes before being submerged in the supplied lysis buffer 4°C overnight in the dark. Slides were then incubated with chilled neutral electrophoresis buffer at 4°C for 30 minutes before being subjected to 21V for 45 minutes. Slides were submerged with DNA precipitation at RT for 30 minutes and then 70% ethanol at RT for 30 minutes. Slides were then dried and stained with 1X SYBR gold as described above. Comets were imaged on a Zeiss Axio Observer using a 10X objective. Comets were quantified using the comet pipeline from CellProfiler. All images within a single experiment were fed into the same pipeline and comets were quantified in an unbiased fashion using the automated program. Extent Tail moment is defined as Tail DNA % multiplied with the length of the comet tail.

Transfections

For RNA interference, cells were incubated with *Silencer*® Select Pre-designed siRNAs for BRD2 (Thermo, s12071), BRD3 (Thermo, s15545), BRD4 (Thermo, 23902), or negative control (Thermo, 4390846). Transfections were done with Lipofectamine RNAiMAX transfection reagent (Invitrogen) according to the manufacturer's protocol and harvested after incubation with siRNA for 72 hours.

For transfection of RNase H1 constructs, cells were transfected with WT RNase H1 (Addgene, 111906), the D210N mutant (Addgene, 111904), or WKKD mutant (Addgene, 111904) which were a gift from Xiang-Dong Fu and previously described[28].

750 fmol of plasmid was incubated with a 6:1 ratio of Xtremegene HP transfection reagent at RT for 20 minutes in 1 mL of Opti-mem media. The transfection mixture was then added dropwise to a 10cm dish containing

Cells at 70% confluence for 24 hours. Cells were then selected with 100 µg/mL hygromycin for 24 hours before fixing (for immunofluorescence experiments) or immediately fixed (for ChIP experiments).

Plasmid Construction

The iBRD4 plasmids were constructed using the pCW57-GFP-2A-MCS backbone (Addgene, 71783), which was a gift from Adam Karpf and previously described[83]. Gibson assembly was used to insert either mCherry-2A-Flag-BRD4 isoform A or isoform C into the backbone in place of the TurboGFP-P2A-hPGK promoter-PuroR-T2A-rTetR region. The C-terminal domain was deleted from isoform A using PCR (AΔCTD). The extra-terminal domain was deleted from isoform C using PCR (CΔET). Sanger sequencing was performed to verify the cloning products.

Small Molecule Inhibitors

The BET protein degrader dBET6 was a gift from Nathanael Gray and previously described[38]. dBET6 was used at a concentration of 100 nM in all experiments except those involving the iBRD4 system, in which it was used at 10 nM. The BET protein inhibitor JQ1 was a gift from James Bradner and previously described[84]. JQ1 was used at a concentration of 500 nM for all experiments. The CDK9 inhibitor DRB (Cayman Chemical Company, 10010302) was used at a concentration of 100 µM for all

experiments. The CDK7 inhibitor triptolide (EMD Millipore, 645900) was used at a concentration of 250 nM (HeLa) or 1 μM (HCT-116).

EdU Detection

EdU detection was done according using the EdU-Click Chemistry 488 kit (Sigma-Aldrich, BCK-EDU488) according to manufacturer's instructions. In brief, cells were pulsed with 10 μM EdU alongside simultaneous treatment with DMSO or dBET6. Cells were then fixed, washed with PBS, and blocked as described above. Cells were then incubated at RT for 30 minutes in the click chemistry cocktail. Following incubation, cells were washed three times with PBS. After the click chemistry was completed, cells were further process according to the immunofluorescence methods described above.

Flow Cytometry and Cell Cycle Analysis

For cell cycle analysis, cells were trypsinized and washed with ice cold PBS. Cells were then fixed with 70% ethanol at 4°C for 30 minutes. Cells were then washed with PBS twice before being incubated with 100 μg/mL RNase A and 50 μg/mL propidium iodide overnight at 4°C. Cells were then quantified by flow cytometry for DNA content on a BD FACSCanto II machine. For analysis, flow results were entered into the univariate cell cycle modeling in FlowJo for the distribution of cell cycle.

For EdU and γH2AX flow experiments, cells were fixed and stained according to the EdU click chemistry and immunofluorescence methods described above. Cells were then quantified for EdU and γH2AX signal on a BD FACSCanto II machine. FlowJo was then used to generate the figures. Cells that were not pulsed with EdU were used as a

negative control for EdU click chemistry. Cells not stained with γH2AX primary antibody were used as a negative control for γH2AX staining.

Chromatin Immunoprecipitation Followed by Next Generation Sequencing (ChIP-seq)

Wild-type HeLa cells (ChIP) or cells transfected with RNase H1 D210N (R-ChIP) were both prepared for qPCR or sequencing using the SimpleChIP® Plus Sonication Chromatin IP Kit according to the manufacturer's instructions. In brief, cells were washed with ice cold PBS and then fixed with 1% formaldehyde in PBS at RT for 13 minutes. The fixation reaction was then halted using a 1X Glycine solution. Cells were then scraped from the plates and pelleted. Cells were then incubated with 1X ChIP sonication cell lysis buffer plus protease inhibitors (PIC) on ice for 10 minutes. Cells were then pelleted and the previous step was repeated. Nuclei were then pelleted and resuspended in ice cold ChIP Sonication Nuclear Lysis buffer with PIC and incubated on ice for 10 minutes. Lysates were then fragmented by sonication with a QSonica Q700 at 4°C for 15 minutes ON-time with a 15s on, 45s off program. After sonication, a sample for 2% input was removed. 10 µg of lysates were then incubated with a ChIP grade antibody at 4°C overnight. 30 uL of magnetic beads were then added to the mixture and incubated at 4°C for two hours before going through a series of salt washes. Chromatin was then eluted from the magnetic beads in the elution buffer at 65°C for 30 minutes while vortexing. The supernatant was removed and treated with RNase A followed by Proteinase K. ChIP DNA was then purified using the supplied columns. Library preparation, Next Generation Sequencing, and analysis was

performed by GeneWiz to determine the level of ChIP-seq or R-ChIP-seq signal following DMSO or dBET6 treatment for two hours. Log2 ratio normalization to input was done using the bamCompare function of deepTools with default inputs.

Chromatin Immunoprecipitation Followed by qPCR (ChIP-qPCR)

DNA for ChIP-qPCR and R-ChIP-qPCR was prepared the same was as described for ChIP-seq experiments. Equal volumes of DNA template were subjected to qPCR with qPCR primers designed against the transcription start sites, exons, introns, and transcription termination sites of candidate genes using iTaq Universal SYBR Green Supermix. Samples were normalized to input to determine the relative amounts of ChIP and R-ChIP signal after DMSO or dBET6 treatment for two hours. Primer sequences can be found in the Source File.

ACKNOWLEDGEMENTS

We thank Xiang-Dong Fu for providing the RNase H1 constructs, Nathanael Gray for providing dBET6, and James Bradner for providing JQ1. We also thank Duke MSTP for providing funding for D.E. to conduct this work. The work was funded by Burroughs Wellcome Career Award for Medical Scientists and American Cancer Society Research Scholar Grant 133394-RSG-19-030-01-DMC to S.R.F.

AUTHOR CONTRIBUTIONS

D.E and S.R.F. designed the project. D.E., R.M., J.P.T., J.P., E.B-S., J.L., and Jin. L. conducted the experiments. D.E., R.M., and S.R.F. analyzed the data. D.E. and S.R.F. wrote the manuscript. All authors read and approved the final version of the manuscript.

REFERENCES

1. Hanahan, D. & Weinberg, R. A. Hallmarks of cancer: the next generation. *Cell* **144,** 646–674 (2011).
2. Blackford, A. N. & Jackson, S. P. ATM, ATR, and DNA-PK: The Trinity at the Heart of the DNA Damage Response. *Mol Cell* **66,** 801–817 (2017).
3. Hamperl, S. & Cimprich, K. A. Conflict Resolution in the Genome: How Transcription and Replication Make It Work. 1–13 (2016). doi:10.1016/j.cell.2016.09.053
4. Cimprich, K. A. & Cortez, D. ATR: an essential regulator of genome integrity. *Nat. Rev. Mol. Cell Biol.* **9,** 616–627 (2008).
5. Sollier, J. & Cimprich, K. A. Breaking bad: R-loops and genome integrity. *Trends in Cell Biology* **25,** 514–522 (2015).
6. Hage, El, A., French, S. L., Beyer, A. L. & Tollervey, D. Loss of Topoisomerase I leads to R-loop-mediated transcriptional blocks during ribosomal RNA synthesis. *Genes Dev.* **24,** 1546–1558 (2010).
7. Garcia-Muse, T. & Aguilera, A. Transcription-replication conflicts: how they occur and how they are resolved. *Nat. Rev. Mol. Cell Biol.* **17,** 553–563 (2016).
8. Gaillard, H. & Aguilera, A. Transcription as a Threat to Genome Integrity. *Annu. Rev. Biochem.* **85,** 291–317 (2016).
9. Aguilera, A. & Gómez-González, B. DNA–RNA hybrids: the risks of DNA breakage during transcription. *Nat Struct Mol Biol* **24,** 439–443 (2017).
10. Schwab, R. A. *et al.* The Fanconi Anemia Pathway Maintains Genome Stability by Coordinating Replication and Transcription. *Mol Cell* **60,** 351–361 (2015).
11. Zeman, M. K. & Cimprich, K. A. Causes and consequences of replication stress. *Nat. Cell Biol.* **16,** 2–9 (2014).
12. Stork, C. T. *et al.* Co-transcriptional R-loops are the main cause of estrogen-induced DNA damage. *eLife* **5,** e17548 (2016).
13. Kotsantis, P. *et al.* Increased global transcription activity as a mechanism of replication stress in cancer. *Nat Commun* **7,** 13087 (2016).
14. Garcia-Muse, T. & Aguilera, A. R Loops: From Physiological to Pathological Roles. *Cell* **179,** 604–618 (2019).
15. Crossley, M. P., Bocek, M. & Cimprich, K. A. R-Loops as Cellular Regulators and Genomic Threats. *Mol Cell* **73,** 398–411 (2019).
16. Costantino, L. & Koshland, D. Genome-wide Map of R-Loop-Induced Damage Reveals How a Subset of R-Loops Contributes to Genomic Instability. *Mol Cell* **71,** 487–497.e3 (2018).
17. Hamperl, S., Bocek, M. J., Saldivar, J. C., Swigut, T. & Cimprich, K. A. Transcription-Replication Conflict Orientation Modulates R-Loop Levels and Activates Distinct DNA Damage Responses. *Cell* **170,** 774–786.e19 (2017).
18. Richard, P. & Manley, J. L. R Loops and Links to Human Disease. *J. Mol. Biol.* (2016). doi:10.1016/j.jmb.2016.08.031
19. Santos-Pereira, J. M. & Aguilera, A. R loops: new modulators of genome dynamics and function. *Nature Reviews Genetics* **16,** 583–597 (2015).
20. Kabeche, L., Nguyen, H. D., Buisson, R. & Zou, L. A mitosis-specific and R loop-driven ATR pathway promotes faithful chromosome segregation. *Science* (2017). doi:10.1126/science.aan6490

21. Shao, W. & Zeitlinger, J. Paused RNA polymerase II inhibits new transcriptional initiation. *Nature Publishing Group* **49,** 1045–1051 (2017).
22. Xiao, Y. *et al.* Structure Basis for Directional R-loop Formation and Substrate Handover Mechanisms in Type I CRISPR-Cas System. *Cell* **170,** 48–60.e11 (2017).
23. Stuckey, R., García-Rodríguez, N., Aguilera, A. & Wellinger, R. E. Role for RNA:DNA hybrids in origin-independent replication priming in a eukaryotic system. *Proc. Natl. Acad. Sci. U.S.A.* **112,** 5779–5784 (2015).
24. Skourti-Stathaki, K. & Proudfoot, N. J. A double-edged sword: R loops as threats to genome integrity and powerful regulators of gene expression. *Genes Dev.* **28,** 1384–1396 (2014).
25. Chaudhuri, J. & Alt, F. W. Class-switch recombination: interplay of transcription, DNA deamination and DNA repair. *Nat. Rev. Immunol.* **4,** 541–552 (2004).
26. Gan, W. *et al.* R-loop-mediated genomic instability is caused by impairment of replication fork progression. *Genes Dev.* **25,** 2041–2056 (2011).
27. Matos, D. A. *et al.* ATR Protects the Genome against R Loops through a MUS81-Triggered Feedback Loop. *Mol Cell* (2019). doi:10.1016/j.molcel.2019.10.010
28. Chen, L. *et al.* R-ChIP Using Inactive RNase H Reveals Dynamic Coupling of R-loops with Transcriptional Pausing at Gene Promoters. *Mol Cell* (2017). doi:10.1016/j.molcel.2017.10.008
29. Zatreanu, D. *et al.* Elongation Factor TFIIS Prevents Transcription Stress and R-Loop Accumulation to Maintain Genome Stability. *MOLCEL* **76,** 57–69.e9 (2019).
30. Wessel, S. R., Mohni, K. N., Luzwick, J. W., Dungrawala, H. & Cortez, D. Functional Analysis of the Replication Fork Proteome Identifies BET Proteins as PCNA Regulators. *Cell Reports* **28,** 3497–3509.e4 (2019).
31. Grunseich, C. *et al.* Senataxin Mutation Reveals How R-Loops Promote Transcription by Blocking DNA Methylation at Gene Promoters. *Mol Cell* **69,** 426–437.e7 (2018).
32. Shivji, M. K. K., Renaudin, X., Williams, Ç. H. & Venkitaraman, A. R. BRCA2 Regulates Transcription Elongation by RNA Polymerase II to Prevent R-Loop Accumulation. *Cell Reports* **22,** 1031–1039 (2018).
33. Parajuli, S. *et al.* Human Ribonuclease H1 resolves R loops and thereby enables progression of the DNA replication fork. *J Biol Chem* jbc.M117.787473–19 (2017). doi:10.1074/jbc.M117.787473
34. Nguyen, H. D. *et al.* Functions of Replication Protein A as a Sensor of R Loops and a Regulator of RNaseH1. *Mol Cell* **65,** 832–847.e4 (2017).
35. Morales, J. C. *et al.* XRN2 Links Transcription Termination to DNA Damage and Replication Stress. *PLoS Genet* **12,** e1006107 (2016).
36. Wahba, L., Amon, J. D., Koshland, D. & Vuica-Ross, M. RNase H and Multiple RNA Biogenesis Factors Cooperate to Prevent RNA:DNA Hybrids from Generating Genome Instability. *MOLCEL* **44,** 978–988 (2011).
37. Skourti-Stathaki, K., Proudfoot, N. J. & Gromak, N. Human senataxin resolves RNA/DNA hybrids formed at transcriptional pause sites to promote Xrn2-dependent termination. *Mol Cell* **42,** 794–805 (2011).

38. Winter, G. E. *et al.* BET Bromodomain Proteins Function as Master Transcription Elongation Factors Independent of CDK9 Recruitment. *Mol Cell* (2017). doi:10.1016/j.molcel.2017.06.004
39. Kanno, T. *et al.* BRD4 assists elongation of both coding and enhancer RNAs by interacting with acetylated histones. *Nat Struct Mol Biol* **21,** 1047–1057 (2014).
40. Itzen, F., Greifenberg, A. K., Bösken, C. A. & Geyer, M. Brd4 activates P-TEFb for RNA polymerase II CTD phosphorylation. *Nucleic Acids Res* **42,** 7577–7590 (2014).
41. Chen, R., Yik, J. H. N., Lew, Q. J. & Chao, S.-H. Brd4 and HEXIM1: multiple roles in P-TEFb regulation and cancer. *Biomed Res Int* **2014,** 232870–11 (2014).
42. Liu, W. *et al.* Brd4 and JMJD6-associated anti-pause enhancers in regulation of transcriptional pause release. *Cell* **155,** 1581–1595 (2013).
43. Patel, M. C. *et al.* BRD4 coordinates recruitment of pause release factor P-TEFb and the pausing complex NELF/DSIF to regulate transcription elongation of interferon-stimulated genes. *Mol. Cell. Biol.* **33,** 2497–2507 (2013).
44. Zhang, W. *et al.* Bromodomain-containing protein 4 (BRD4) regulates RNA polymerase II serine 2 phosphorylation in human CD4+ T cells. *J Biol Chem* **287,** 43137–43155 (2012).
45. Rahman, S. *et al.* The Brd4 extraterminal domain confers transcription activation independent of pTEFb by recruiting multiple proteins, including NSD3. *Mol. Cell. Biol.* **31,** 2641–2652 (2011).
46. Jang, M. K. *et al.* The Bromodomain Protein Brd4 Is a Positive Regulatory Component of P-TEFb and Stimulates RNA Polymerase II-Dependent Transcription. *Mol Cell* **19,** 523–534 (2005).
47. Muhar, M. *et al.* SLAM-seq defines direct gene-regulatory functions of the BRD4-MYC axis. *Science* **360,** 800–805 (2018).
48. Delmore, J. E. *et al.* BET bromodomain inhibition as a therapeutic strategy to target c-Myc. *Cell* **146,** 904–917 (2011).
49. Filippakopoulos, P. *et al.* Selective inhibition of BET bromodomains. *Nature* **468,** 1067–1073 (2010).
50. Filippakopoulos, P. *et al.* Histone recognition and large-scale structural analysis of the human bromodomain family. *Cell* **149,** 214–231 (2012).
51. Floyd, S. R. *et al.* The bromodomain protein Brd4 insulates chromatin from DNA damage signalling. *Nature* **498,** 246–250 (2013).
52. Rathert, P. *et al.* Transcriptional plasticity promotes primary and acquired resistance to BET inhibition. *Nature* **525,** 543–547 (2015).
53. Asangani, I. A. *et al.* Therapeutic targeting of BET bromodomain proteins in castration-resistant prostate cancer. *Nature* **510,** 278–282 (2014).
54. Zuber, J. *et al.* RNAi screen identifies Brd4 as a therapeutic target in acute myeloid leukaemia. *Nature* **478,** 524–528 (2011).
55. Dawson, M. A. *et al.* Inhibition of BET recruitment to chromatin as an effective treatment for MLL-fusion leukaemia. *Nature* **478,** 529–533 (2011).
56. Floyd, S. R. *et al.* The bromodomain protein Brd4 insulates chromatin from DNA damage signalling. *Nature* **498,** 246–250 (2013).
57. Zhang, J. *et al.* BRD4 facilitates replication stress-induced DNA damage response. *Oncogene* **37,** 3763–3777 (2018).

58. Sun, C. *et al.* BRD4 Inhibition Is Synthetic Lethal with PARP Inhibitors through the Induction of Homologous Recombination Deficiency. *Cancer Cell* **33,** 401–416.e8 (2018).
59. Bowry, A., Piberger, A. L., Rojas, P., Saponaro, M. & Petermann, E. BET Inhibition Induces HEXIM1- and RAD51-Dependent Conflicts between Transcription and Replication. *Cell Reports* **25,** 2061–2069.e4 (2018).
60. Schröder, S. *et al.* Two-pronged binding with bromodomain-containing protein 4 liberates positive transcription elongation factor b from inactive ribonucleoprotein complexes. *J Biol Chem* **287,** 1090–1099 (2012).
61. Rogakou, E. P., Pilch, D. R., Orr, A. H., Ivanova, V. S. & Bonner, W. M. DNA double-stranded breaks induce histone H2AX phosphorylation on serine 139. *J Biol Chem* **273,** 5858–5868 (1998).
62. Maruyama, T. *et al.* A Mammalian bromodomain protein, brd4, interacts with replication factor C and inhibits progression to S phase. *Mol. Cell. Biol.* **22,** 6509–6520 (2002).
63. Zhou, Y., Zhou, J., Lu, X., Tan, T.-Z. & Chng, W.-J. BET Bromodomain inhibition promotes De-repression of TXNIP and activation of ASK1-MAPK pathway in acute myeloid leukemia. *BMC Cancer* **18,** 731–11 (2018).
64. Fiskus, W. *et al.* Highly active combination of BRD4 antagonist and histone deacetylase inhibitor against human acute myelogenous leukemia cells. *Mol. Cancer Ther.* **13,** 1142–1154 (2014).
65. Olson, E., Nievera, C. J., Klimovich, V., Fanning, E. & Wu, X. RPA2 is a direct downstream target for ATR to regulate the S-phase checkpoint. *J Biol Chem* **281,** 39517–39533 (2006).
66. Pivot-Pajot, C. *et al.* Acetylation-dependent chromatin reorganization by BRDT, a testis-specific bromodomain-containing protein. *Mol. Cell. Biol.* **23,** 5354–5365 (2003).
67. Maruyama, T. *et al.* A Mammalian bromodomain protein, brd4, interacts with replication factor C and inhibits progression to S phase. *Mol. Cell. Biol.* **22,** 6509–6520 (2002).
68. Bisgrove, D. A., Mahmoudi, T., Henklein, P. & Verdin, E. Conserved P-TEFb-interacting domain of BRD4 inhibits HIV transcription. *Proc. Natl. Acad. Sci. U.S.A.* **104,** 13690–13695 (2007).
69. Chen, J.-Y., Zhang, X., Fu, X.-D. & Chen, L. R-ChIP for genome-wide mapping of R-loops by using catalytically inactive RNASEH1. *Nat Protoc* **46,** 115 (2019).
70. Krueger, B. J., Varzavand, K., Cooper, J. J. & Price, D. H. The mechanism of release of P-TEFb and HEXIM1 from the 7SK snRNP by viral and cellular activators includes a conformational change in 7SK. *PLoS ONE* **5,** e12335 (2010).
71. Sollier, J. *et al.* Transcription-Coupled Nucleotide Excision Repair Factors Promote R-Loop-Induced Genome Instability. *Mol Cell* **56,** 777–785 (2014).
72. Li, X. & Manley, J. L. Inactivation of the SR protein splicing factor ASF/SF2 results in genomic instability. *Cell* **122,** 365–378 (2005).
73. Porrua, O. & Libri, D. Transcription termination and the control of the transcriptome: why, where and how to stop. *Nature Publishing Group* **16,** 190–202 (2015).

74. Haberle, V. & Stark, A. Eukaryotic core promoters and the functional basis of transcription initiation. *Nature Publishing Group* **19,** 621–637 (2018).
75. Komarnitsky, P., Cho, E. J. & Buratowski, S. Different phosphorylated forms of RNA polymerase II and associated mRNA processing factors during transcription. *Genes Dev.* **14,** 2452–2460 (2000).
76. Baumli, S., Hole, A. J., Wang, L.-Z., Noble, M. E. M. & Endicott, J. A. The CDK9 Tail Determines the Reaction Pathway of Positive Transcription Elongation Factor b. *Structure/Folding and Design* **20,** 1788–1795 (2012).
77. Shao, W. & Zeitlinger, J. Paused RNA polymerase II inhibits new transcriptional initiation. *Nature Publishing Group* **49,** 1045–1051 (2017).
78. LeRoy, G., Rickards, B. & Flint, S. J. The double bromodomain proteins Brd2 and Brd3 couple histone acetylation to transcription. *Mol Cell* **30,** 51–60 (2008).
79. Hsu, S. C. *et al.* The BET Protein BRD2 Cooperates with CTCF to Enforce Transcriptional and Architectural Boundaries. *Mol Cell* **66,** 102–116.e7 (2017).
80. Cheung, K. L. *et al.* Distinct Roles of Brd2 and Brd4 in Potentiating the Transcriptional Program for Th17 Cell Differentiation. *Mol Cell* **65,** 1068–1080.e5 (2017).
81. Houzelstein, D. *et al.* Growth and early postimplantation defects in mice deficient for the bromodomain-containing protein Brd4. *Mol. Cell. Biol.* **22,** 3794–3802 (2002).
82. Bolden, J. E. *et al.* Inducible in vivo silencing of Brd4 identifies potential toxicities of sustained BET protein inhibition. *Cell Reports* **8,** 1919–1929 (2014).
83. Barger, C. J., Branick, C., Chee, L. & Karpf, A. R. Pan-Cancer Analyses Reveal Genomic Features of FOXM1 Overexpression in Cancer. *Cancers (Basel)* **11,** (2019).
84. Filippakopoulos, P. *et al.* Selective inhibition of BET bromodomains. *Nature* **468,** 1067–1073 (2010).

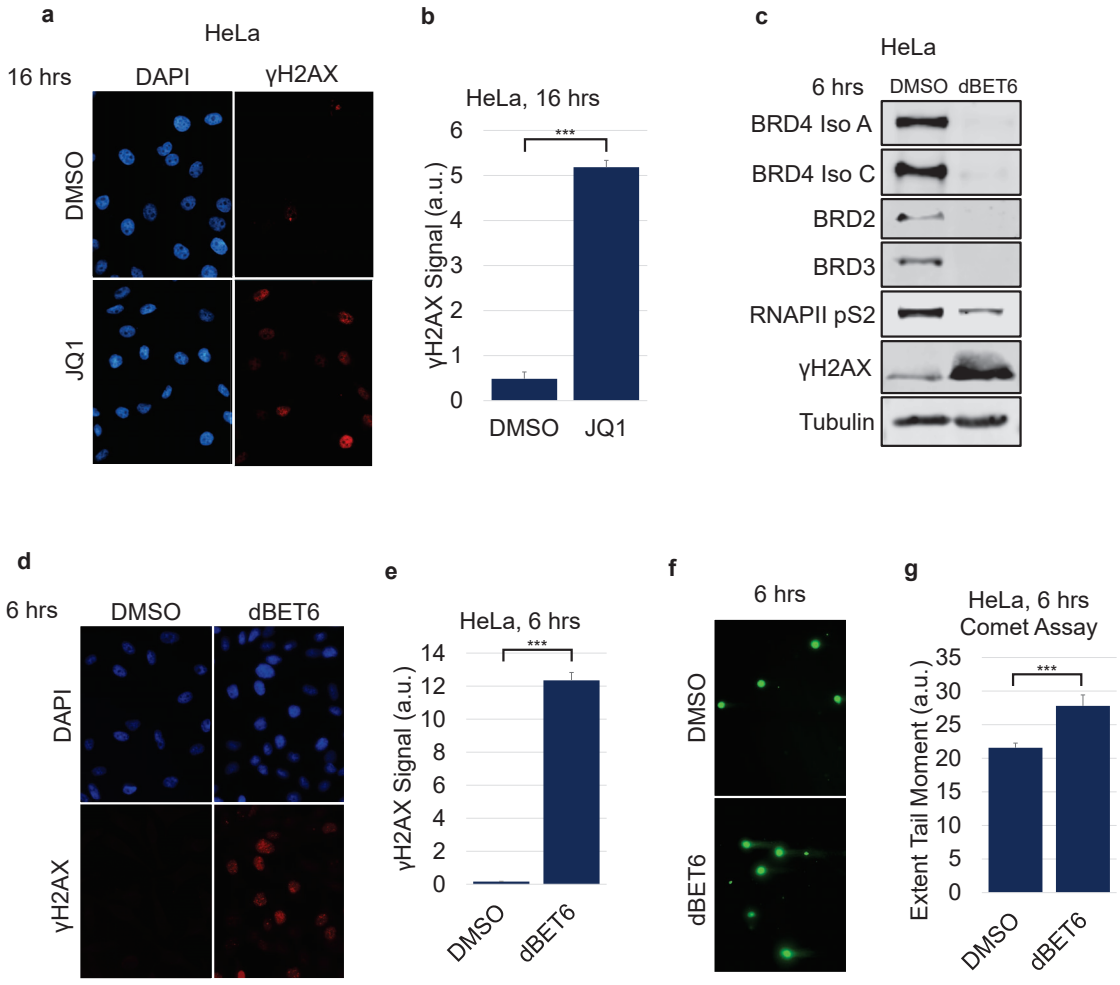

Figure 1

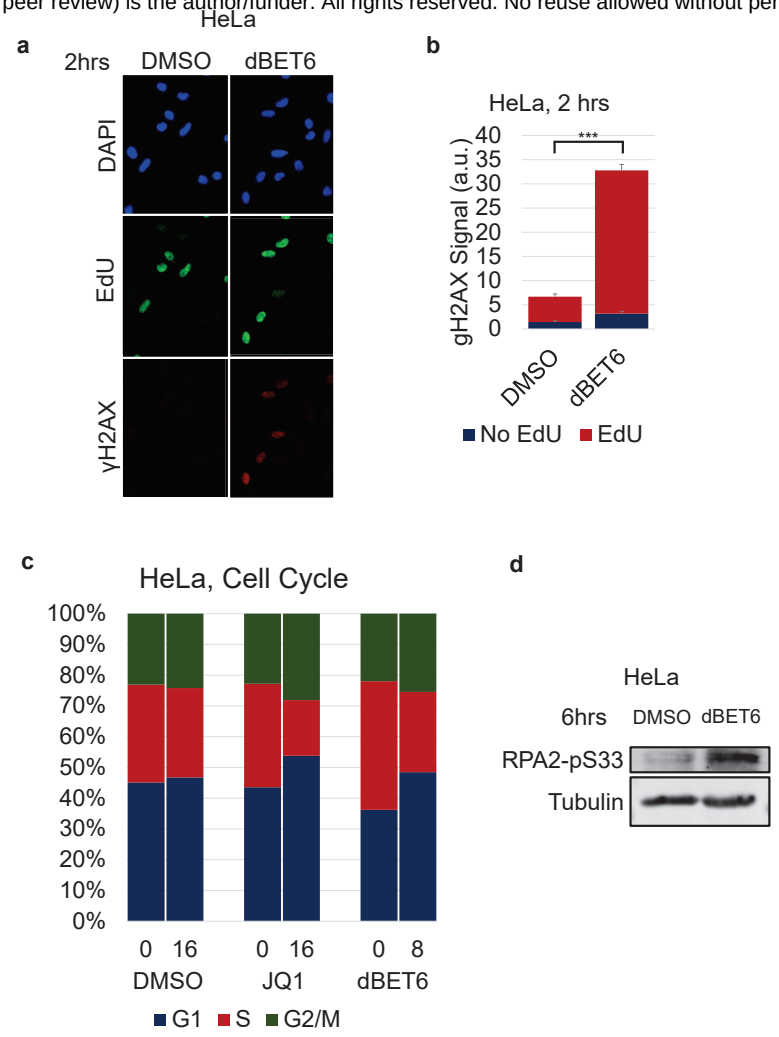

Figure 2

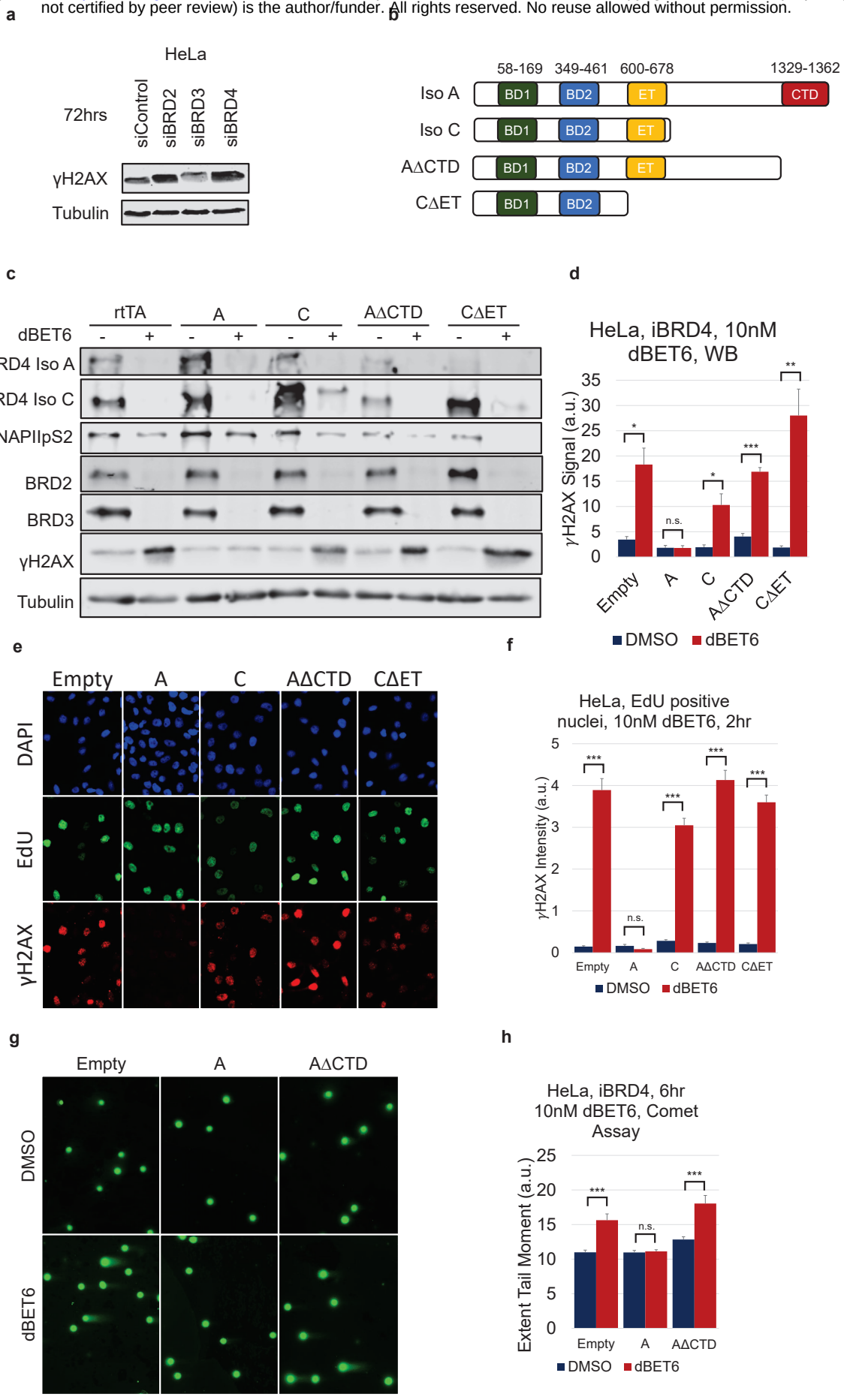

Figure 3

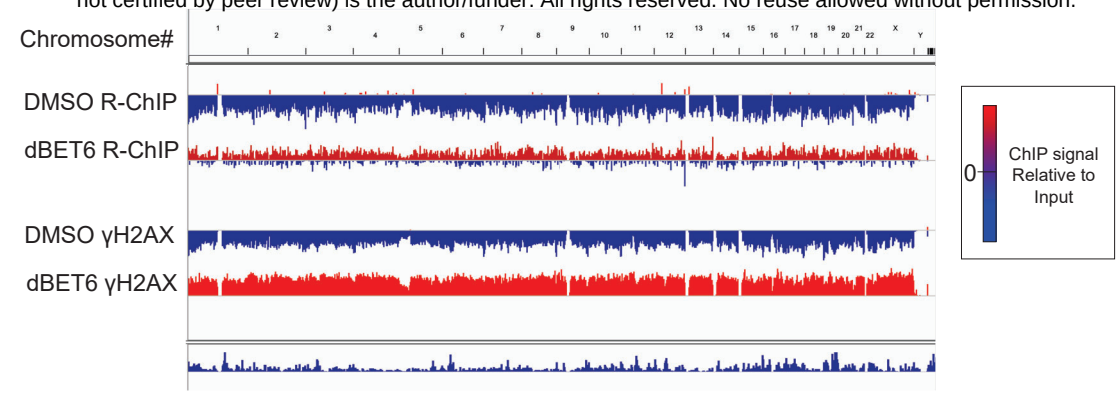

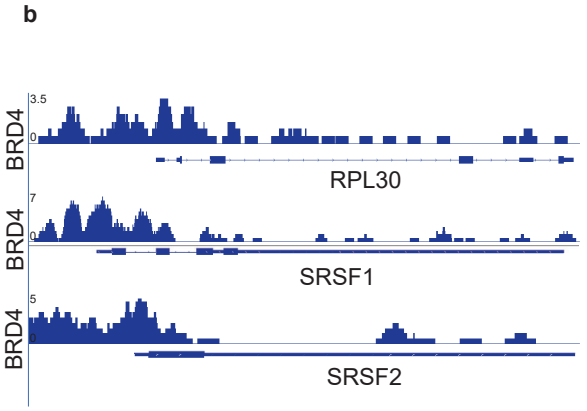

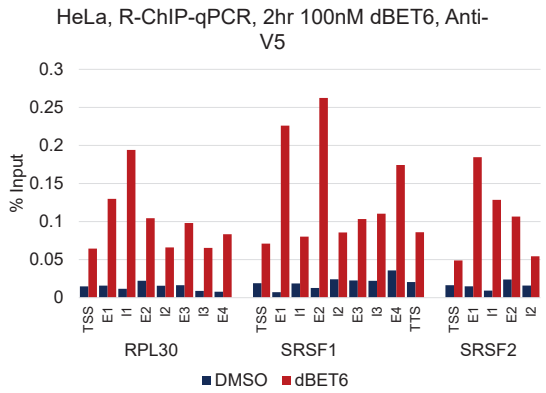

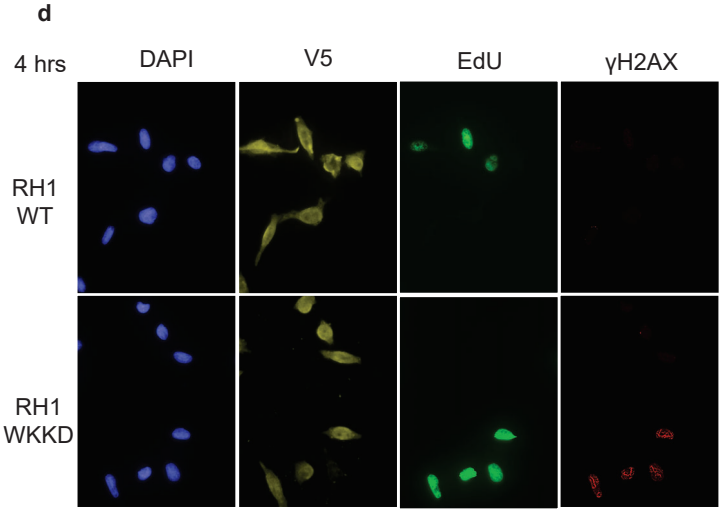

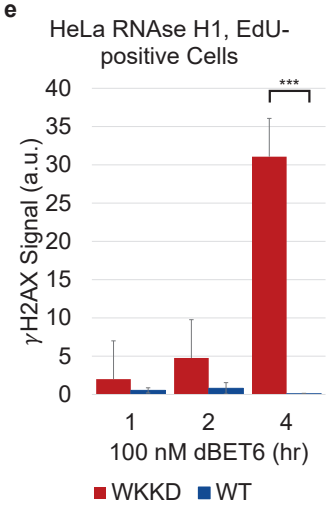

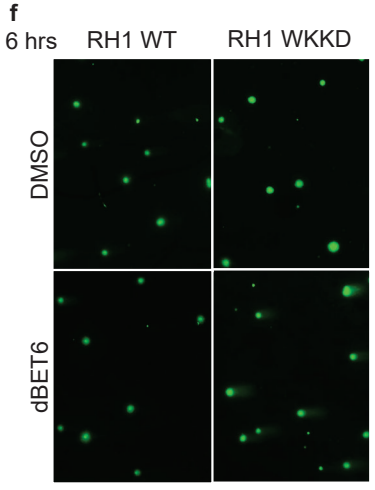

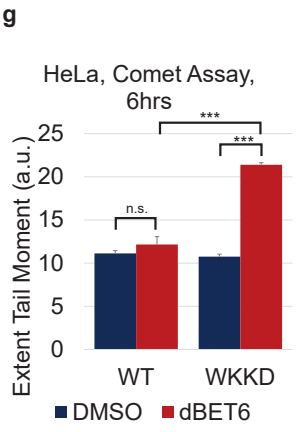

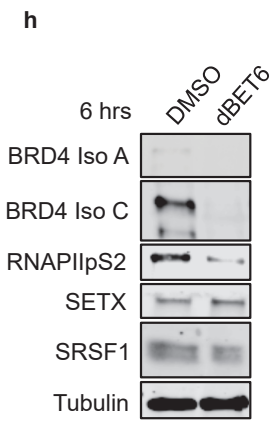

Figure 4

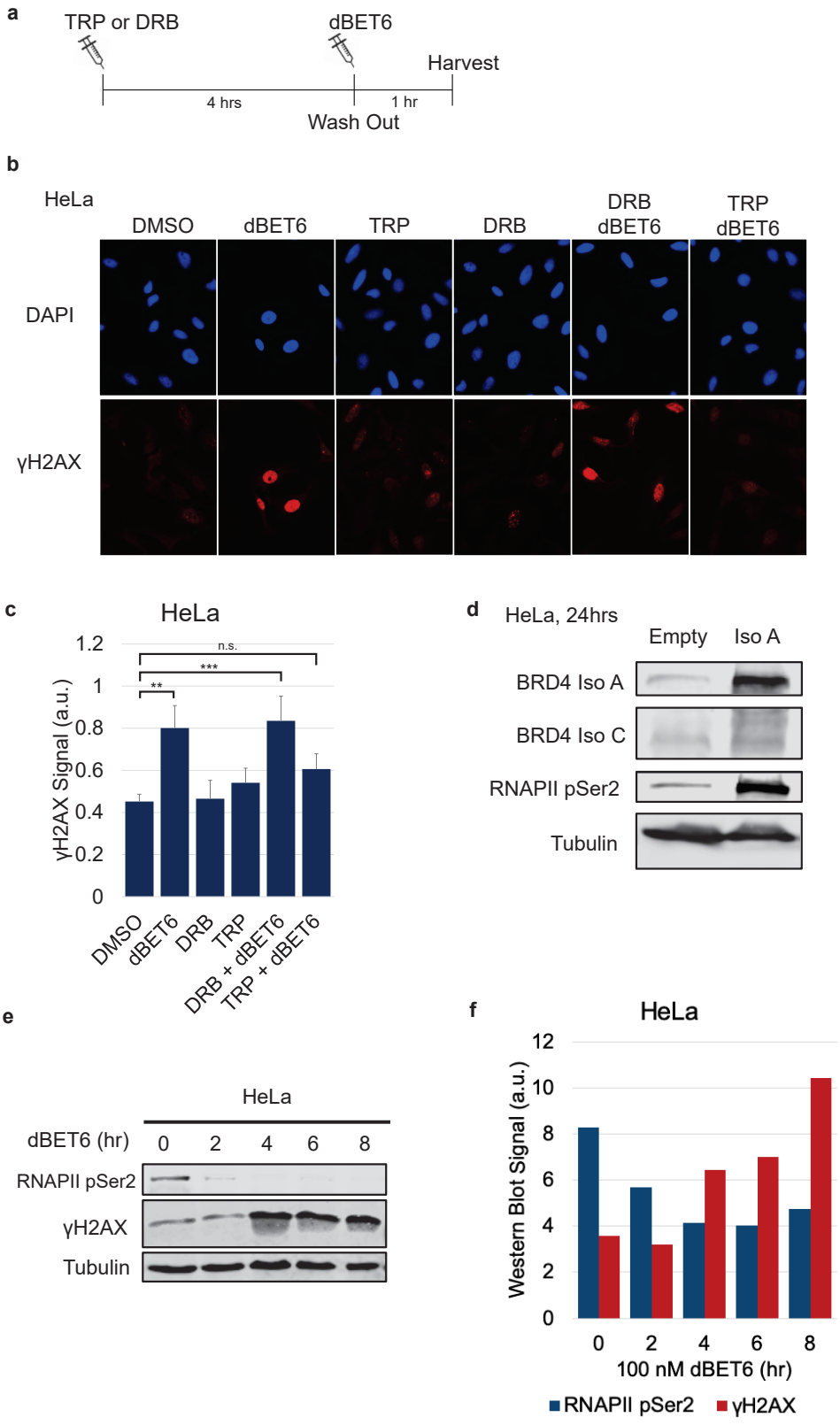

Figure 5

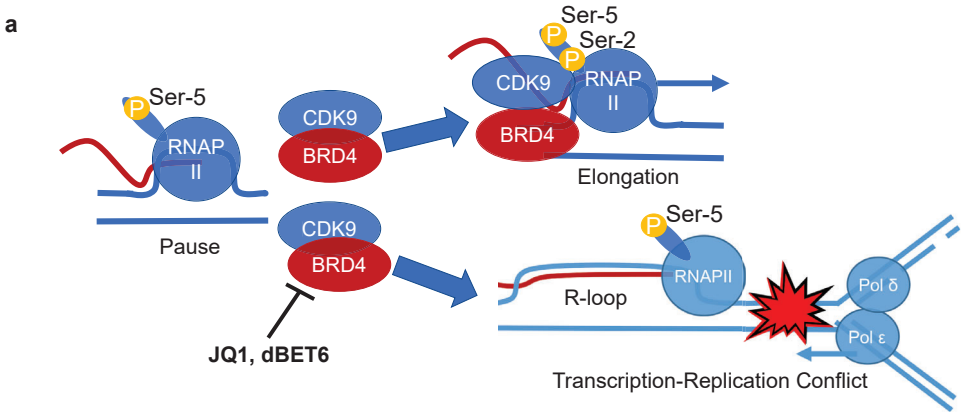

Figure 6

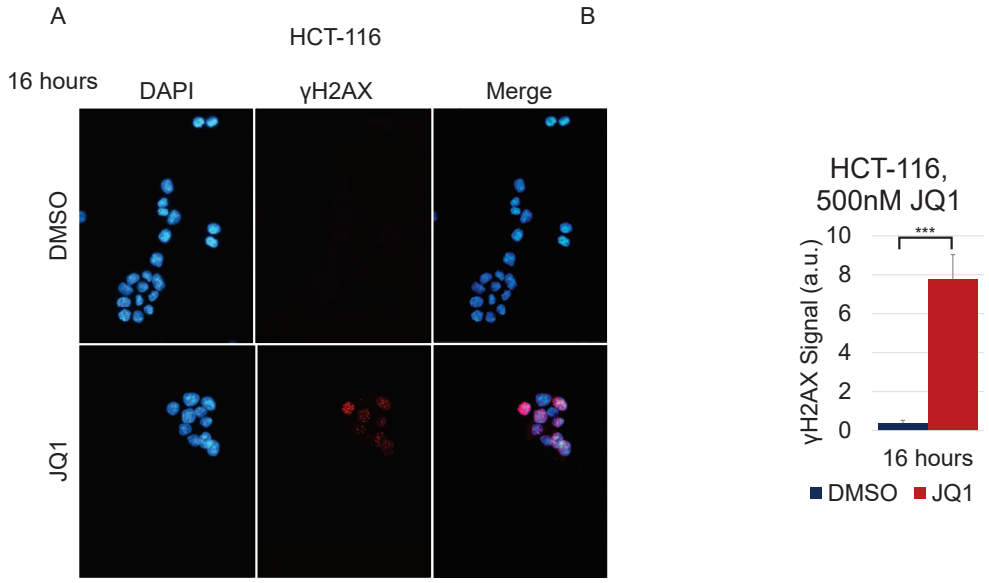

Figure S1

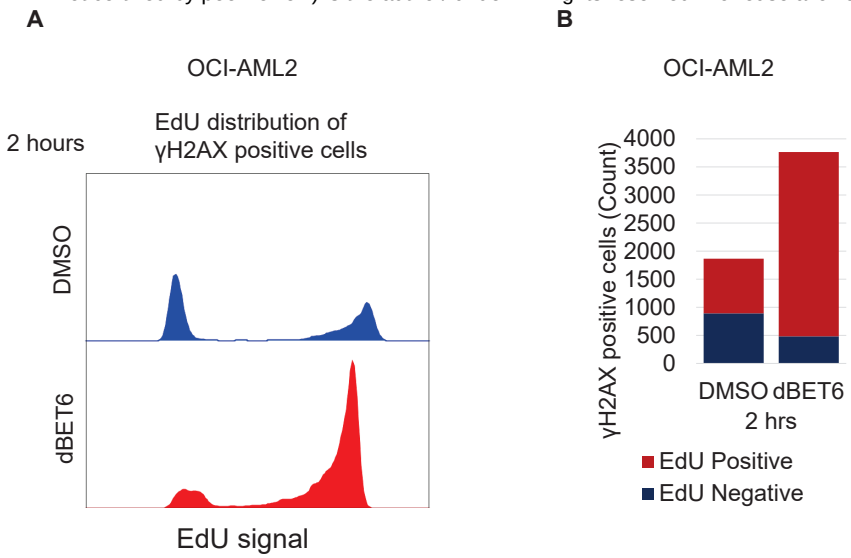

Figure S2

A

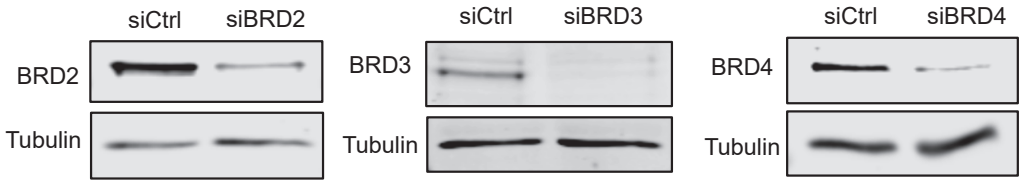

B

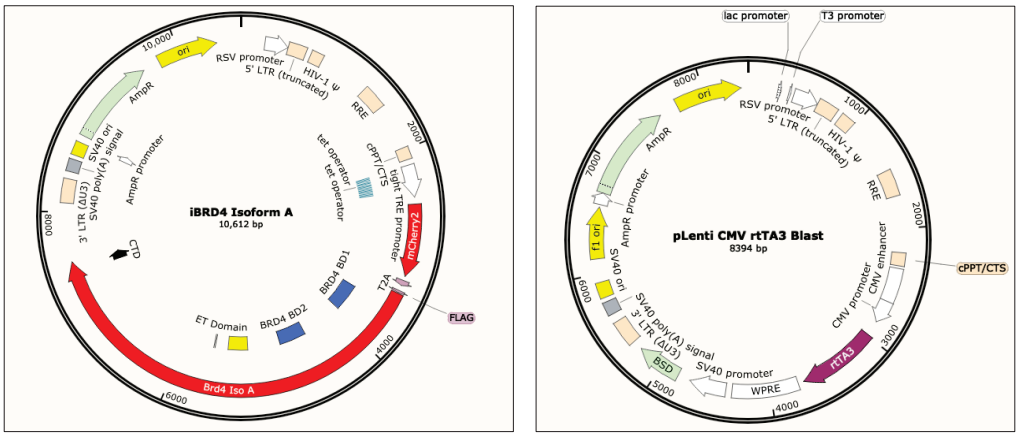

C

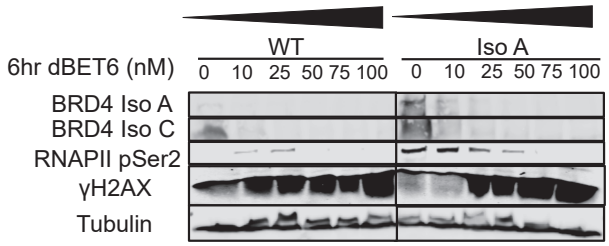

D

HeLa, Isoform A overexpression, 24hrs Doxycycline, Before sorting

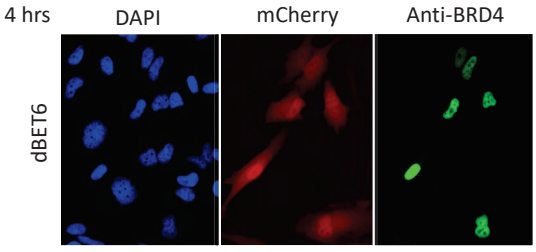

E

HeLa, Isoform C overexpression, 24hrs Doxycycline, Before sorting

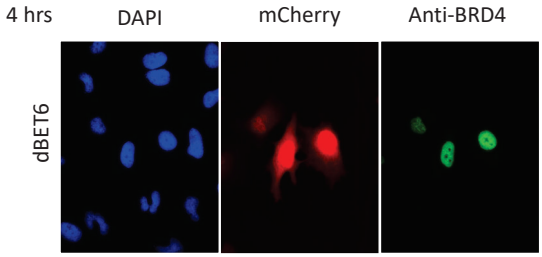

Figure S3

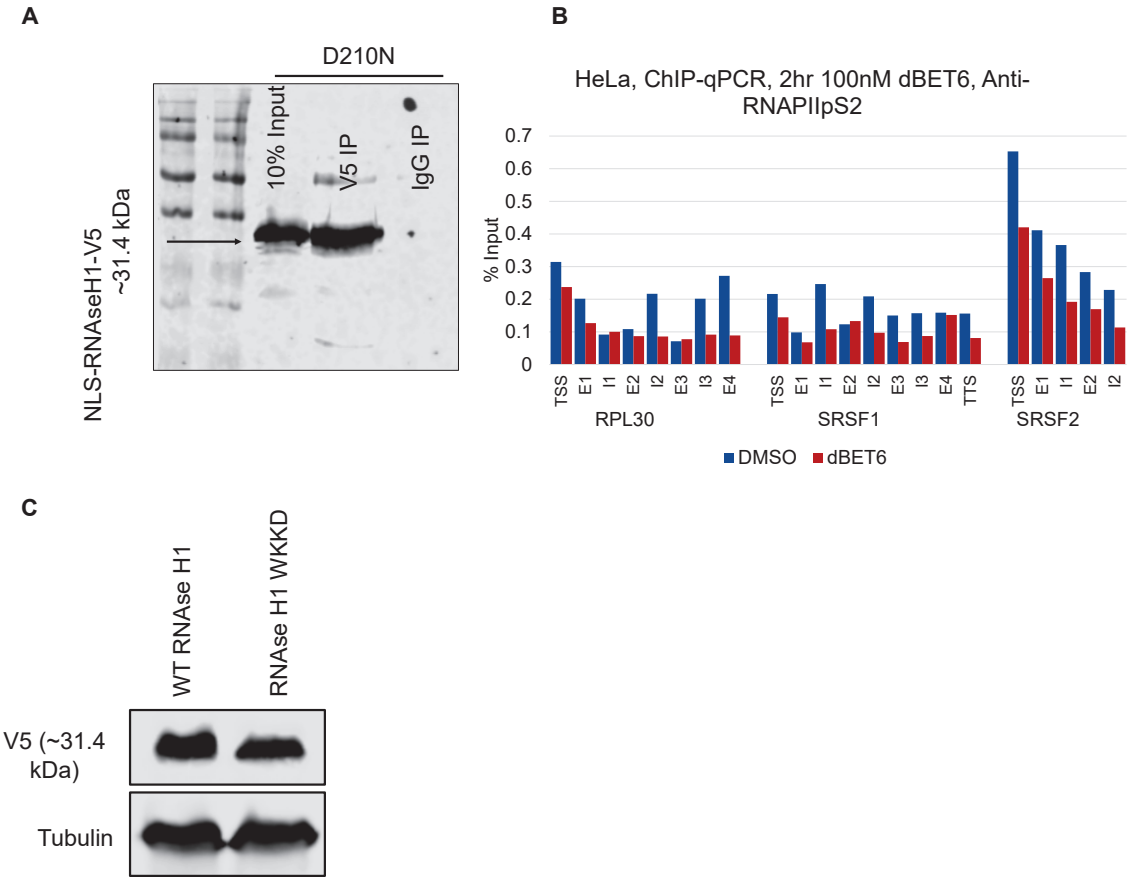

Figure S4

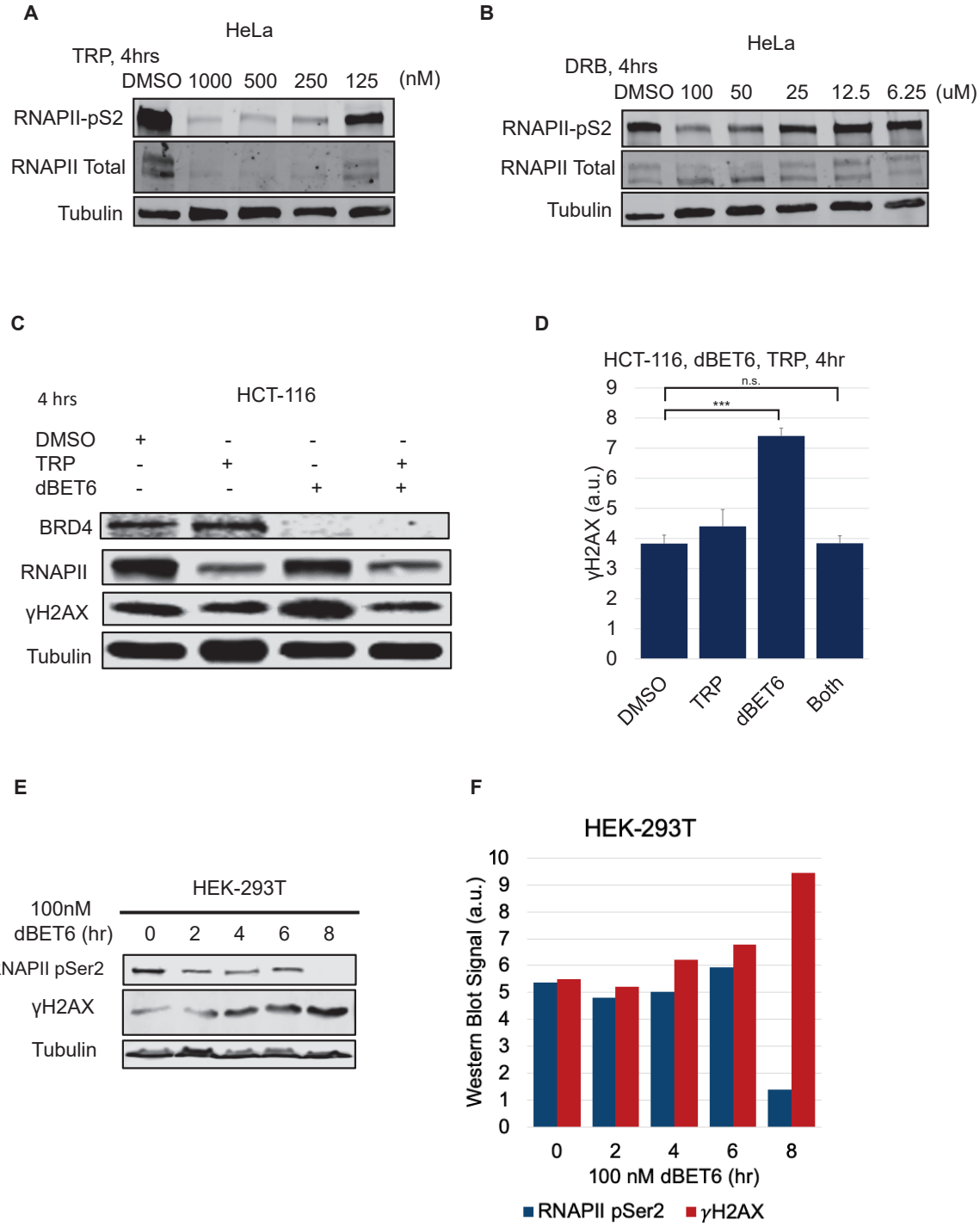

Figure S5